Lifetime Control of Electromechanical Actuators

Levent U. Gökdere[1], Stephen L. Chiu[1], Kirby J. Keller[2], John Vian[3]

[1]Rockwell Scientific
1049 Camino Dos Rios
Thousand Oaks, CA 91360
lgokdere@rwsc.com
schiu@rwsc.com

[2]Boeing Company
P.O. Box 516
St. Louis, MO 63166
kirby.j.keller@boeing.com

[3]Boeing Company
P.O. Box 3707, MC 45-85
Seattle, WA 98124
john.vian@boeing.com

Abstract— Existing actuator controls are typically designed based on optimizing performance and robustness to system uncertainties, without considering the operational lifetime of the actuator. It is often desirable, and sometimes necessary, to trade off performance for extended actuator operational lifetime. This paper introduces the concept of incorporating the actuator lifetime as a controlled parameter. We describe preliminary methods for speed/position tracking control of an electromechanical actuator (EMA) while maintaining a desired minimum lifetime of the actuator motor.

TABLE OF CONTENTS

1. INTRODUCTION

The harder an actuator is pushed to its performance limit, the shorter its lifetime becomes. Existing actuator controllers are typically designed based on optimizing performance and robustness, without considering the operational lifetime of the actuator. It is often desirable, and sometimes necessary, to trade off performance for extended lifetime. For example, the performance of flight actuators on a damaged aircraft is not as important as ensuring that the remaining actuators continue operation until the aircraft can land safely. Similarly, logistic problems may require extending the operational lifetime of a set of actuators until maintenance service or spare parts are available.

This paper introduces the concept of incorporating the actuator lifetime as a controlled parameter. The ability to actively control the actuator's lifetime can extend actuator life, reduce maintenance cost, and improve aircraft safety and mission readiness. In particular, we explore how the desired lifetime of a brushless DC motor in an electromechanical actuator (EMA) can be integrated into the actuator's feedback control law.

Active control of the lifetime of a particular component can be achieved by the following steps: (1) estimation of the residual lifetime (remaining time to failure) based on the component's past operating conditions; and (2) control adaptation to modify the component's current operating condition if the estimated residual lifetime is less than the desired residual lifetime. Control adaptation may include possible modifications to the reference motion trajectory and/or reducing the permissible range of certain internal parameters.

Failures of brushless DC (BLDC) motors are largely due to failure of either the motor winding or motor bearing. In this work, the remaining lifetime of the motor winding is estimated from past motor temperature history, while the remaining lifetime of the motor bearing is estimated from the past load and speed history. Control of motor lifetime is achieved by implementing a linear quadratic (LQ) optimal controller for speed/position tracking control with a lifetime-dependent constraint imposed on the output of the control law [1]. The objective of the controller is to follow the commanded reference speed/position trajectory as closely as possible while satisfying the desired residual lifetime of the motor winding and bearing.

In the following sections, we present methods for predicting the residual lifetime of the BLDC motor, derivation of the lifetime-based control law, and simulation results comparing a standard controller with a lifetime-based controller.

2. PREDICTION OF MOTOR LIFETIME

The primary failure modes of BLDC motors are winding insulation failure and bearing failure. For induction motors, breakage of rotor bars due to mechanical fatigue is also an important failure mode. In [2], on-line recursive least-squares estimation algorithms for detection of electrical and mechanical faults in BLDC motors are described. In this section, we use heuristic methods to develop analytic models for estimating the life expectancy of the motor winding and bearing. These two components are assumed to be initially

0-7803-8870-4/05/$20.00© 2005 IEEE
IEEEAC paper #1288, Version 2, Updated December 10, 2004

fault-free and the objective is to predict the time at which the first sign of fault would occur.

Motor Winding Lifetime Prediction

The life expectancy of motor winding insulation is a function of the winding temperature; different classes of insulation material offer different temperature ratings. For example, typical BLDC motors use class H winding insulation, which provides an average life expectancy of approximately 30,000 hours at 180ºC [3]. The average life expectancy of class H insulation is reduced approximately by half for every 10ºC rise in temperature [3]. Because of the strong influence of temperature on insulation life, most servo motors provide an embedded thermal switch to prevent thermal damage. Aside from mechanisms to reduce bearing wear (e.g., improve motor-load alignment, maintain proper lubrication, reduce electrically induced bearing currents), the best way to prolong motor life is to control its winding temperature.

A typical insulation life expectancy versus temperature curve is shown in Fig. 1. Such data allows us to calculate the expected remaining life of the insulation when the motor operates at a constant temperature (e.g., constant duty operation). However, no formula exists for calculating the remaining life when the winding temperature is varying. We use a heuristic method based on applying Fig. 1 and the assumption that deteriorations incurred at different temperatures are linearly additive. For example, suppose class H insulation (which has a life of 30,000 hours at 180ºC) is operated for 15,000 hours at 180ºC, the remaining lifetime would be 50% (i.e., we can view the insulation as 50% deteriorated). If the operating temperature is subsequently raised to 200ºC, where Fig. 1 indicates the life expectancy of brand new insulation is 5,000 hours, then we estimate the remaining life of the used insulation at 200ºC as 50% x 5,000 hours = 2,500 hours. If the insulation then operates for 1,000 hours at 200ºC, the remaining life is

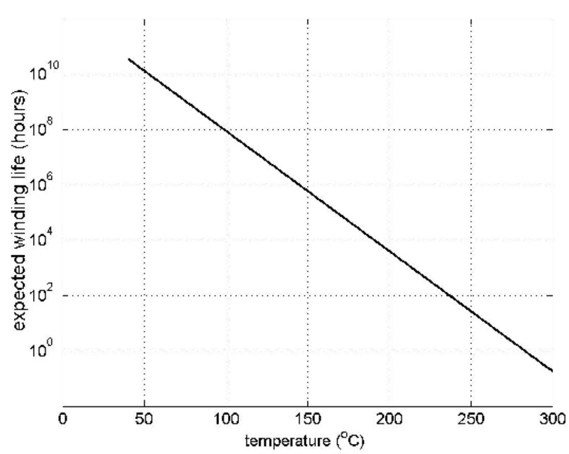

Figure 1 – Typical winding insulation life versus temperature curve.

2,500 – 1,000 = 1,500 hours at 200ºC. The remaining life at 200ºC as a percentage of the life of brand new insulation would be 1,500/5,000 = 30%. The percentage of life expended at each temperature level can be thus calculated and accumulated to estimate the remaining life at any time instant. Since the residual life in terms of absolute hours varies with the operating temperature, residual life tracked as a percentage of full life is more useful. At any instant, we can convert the percentage residual life into absolute residual life-hours for the current operating temperature.

We can also derive the residual life through an alternative calculation. Note that operating for 15,000 hours at 180ºC would wear out 15,000/30,000 = 50% of a new insulation, and operating for 1,000 hours at 200ºC would wear out 1,000/5,000 = 20% of a new insulation. Thus, the sum of the effects of operating for 15,000 hours at 180ºC plus operating for 1,000 hours at 200ºC is to wear out 50% + 20% = 70% of a new insulation. The residual life is then 100% – 70% = 30% of a new insulation.

Specifically, the percentage residual (remaining) life at time instant t is calculated by

$$\%Liferes(t) = 100 \cdot \left(1 - \int_{t_o}^{t} \frac{d\tau}{Life(\tau)}\right), \quad t_o \le \tau < t \tag{1}$$

where t_o is the initial time instant and $Life(\tau)$ is the life expectancy of brand new insulation corresponding to the winding temperature at time instant τ for $t_o \le \tau < t$. Note that $Life(\tau)$ is obtained from the curve in Fig. 1. The integration term in Eq. (1), which is the fractional used life at time instant t, is limited between 0 and 1, and its initial value at time instant t_o is assumed to be zero. The percentage residual lifetime can be converted into absolute residual lifetime at time instant t by

$$Liferes(t) = \frac{\%Liferes(t)}{100} \cdot Life(t) \tag{2}$$

Again, $Life(t)$ in Eq. (2) is the life expectancy of new insulation corresponding to the winding temperature at time instant t.

Motor Thermal Model

Now that we have a method for estimating the residual life of the winding based on winding temperature history, we can develop lifetime control by integrating winding temperature into the control problem formulation. This requires relating winding temperature to the control input, i.e., motor current.

A simple second-order thermal model for estimating the winding temperature of BLDC motors is given in [3]. The thermal model of the BLDC motor can be represented by the equivalent circuit shown in Fig. 2. In this figure, R_{wc} is the

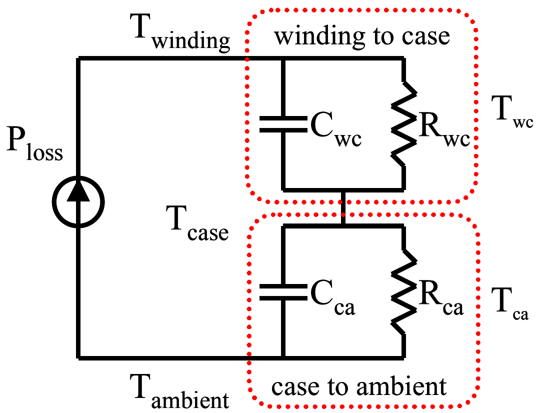

Figure 2 – Equivalent circuit for motor thermal model.

thermal resistance from winding to case, R_{ca} is the thermal resistance from case to ambient air, C_{wc} is the thermal capacitance from winding to case, C_{ca} is the thermal capacitance from case to ambient air, $T_{winding}$ is the winding temperature, T_{case} is the case temperature, $T_{ambient}$ is the ambient air temperature, and P_{loss} is the total power dissipated as heat, which might be approximated by the total copper losses in the windings [3]. A method for on-line estimation of motor thermal model parameters is described in [4].

Motor Bearing Lifetime Prediction

The rated life of motor bearings is commonly specified by the bearing manufacturer in terms of the L10 life – the time duration at which there is a 10% probability of fatigue failure under a given constant load [5]. The fatigue failure occurs in the form of metal chips breaking off from the surface of bearing races or rolling elements – a condition referred to as "spalling."

In its basic form, the L10 life of a motor bearing is specified in terms of number of revolutions that can be attained before 10% of identical bearings would fail. The L10 life can be translated into number of hours by dividing the number of revolutions by the bearing's rotational speed, and is given by

$$L_{10} = \left(\frac{C_r}{P_{eq}}\right)^3 \frac{10^6 \cdot 2\pi}{3600 \cdot \omega_r} \tag{3}$$

where C_r is the bearing's radial load rating specified by the manufacturer (in lbf or N), P_{eq} is the equivalent radial load applied to the bearing, and ω_r is the angular speed of the motor rotor (or, the rotational speed of the bearing inner race) in rad/s. It is important to observe from Eq. (3) that a small change in applied load results in a large change in lifetime. For example, reducing the load by half results in increasing the lifetime by approximately tenfold. In (3), P_{eq} and ω_r are assumed to be positive quantities; otherwise, their absolute values are used.

The L10 life established by bearing manufacturers is based on a constant applied load. For time-varying load, we will estimate the L10 life by using the same heuristics as for winding lifetime prediction; that is, we assume that deteriorations incurred at different load levels are linearly additive. The predicted percentage and absolute residual lifetimes of the motor bearing at time instant t can then be calculated, respectively, by:

$$\%L_{10res}(t) = 100 \cdot \left(1 - \int_{t_o}^{t} \frac{d\tau}{L_{10}(\tau)}\right), \quad t_o \le \tau < t \tag{4}$$

$$L_{10res}(t) = \frac{\%L_{10res}(t)}{100} \cdot L_{10}(t) \tag{5}$$

where $L_{10}(\tau)$ is the life expectancy of brand new bearing corresponding to the radial load and motor speed at time instant τ for $t_o \le \tau < t$. Note that $L_{10}(\tau)$ is obtained from Eq. (3). $L_{10}(t)$ in Eq. (5) is the life expectancy of brand new bearing corresponding to the radial load and motor speed at time instant t.

The linear damage rule (or, the Palmgren-Miner rule) is explained in [5] for bearing life prediction with step changes in load and speed. Equations (4) and (5) are the extended continuous version of the linear damage rule.

From the Weibull plot [6], the bearing life with 50% probability of failure and 90% probability of failure can be approximated, respectively, by

$$L_{50} \approx 5 \cdot L_{10} \tag{6}$$

$$L_{90} \approx 20 \cdot L_{10} \tag{7}$$

where L_{10} is calculated from Eq. (3). Equations (6) and (7) can be used if one wishes to focus on predicted residual life at higher probabilities of failure.

3. Control of Motor Lifetime

Active control of the lifetime of the BLDC motor can be achieved by controlling the operating conditions of the motor winding (i.e., temperature) and bearing (i.e., bearing load or bearing rotational speed). However, the controller must balance the need for extended lifetime with the need to provide good speed/position tracking performance. In this section, we present lifetime control methods based on the linear quadratic (LQ) optimal control framework.

Dynamic Model of BLDC Motor in an EMA

In an EMA, the rotary motion of the BLDC motor is converted into linear motion by coupling the motor shaft to a lead screw through a series of gears. The angular speed of the lead screw ω and the angular speed of the motor ω_r are related by

$$\omega = \frac{\omega_r}{G_{ratio}} \tag{8}$$

where G_{ratio} is the gear reduction ratio (gear box ratio).

A linear dynamic model for such BLDC motor can be given by

$$\dot{X} = AX + bu + d \tag{9}$$

where

$$X = \begin{bmatrix} x_1 \\ x_2 \end{bmatrix} = \begin{bmatrix} \theta_r \\ \omega_r \end{bmatrix}, \tag{10}$$

$$A = \begin{bmatrix} a_{11} & a_{12} \\ a_{21} & a_{22} \end{bmatrix} = \begin{bmatrix} 0 & 1 \\ 0 & \dfrac{-f_m}{J_{total}} \end{bmatrix}, \tag{11}$$

$$b = \begin{bmatrix} b_1 \\ b_2 \end{bmatrix} = \begin{bmatrix} 0 \\ \dfrac{K_T}{J_{total}} \end{bmatrix}, \qquad d = \begin{bmatrix} d_1 \\ d_2 \end{bmatrix} = \begin{bmatrix} 0 \\ \dfrac{-T_L}{J_{total}} \end{bmatrix}. \tag{12}$$

where θ_r is the angular position of the motor in radians, ω_r is the angular speed of the motor in rad/s, u is the torque current of the BLDC motor, which is equal to the current of the conducting phases for the standard 6-step operation of a star-connected BLDC motor (see [7] for BLDC motor torque generation and operation), f_m is the motor friction coefficient in N·m·s/rad, K_t is the torque constant of the motor in N·m/A,

$$J_{total} = J_{mg} + \frac{J_{dsg}}{G_{ratio}^2} + \frac{m}{G_{ratio}^2 \cdot \eta_{ds}} \cdot \frac{DSlead^2}{(2\pi)^2} \tag{13}$$

is the total inertia of the motor and drive screw system in kg·m^2, and

$$T_L = \frac{DSlead}{G_{ratio} \cdot \eta_{ds} \cdot 2\pi} \cdot F_{load} \tag{14}$$

is the load torque acting on the motor shaft in N·m.

In Eqs. (13) and (14), J_{mg} is the total inertia of the motor (rotor and shaft) and motor gear, J_{dsg} is the total inertia of the drive screw and drive screw gear, G_{ratio} is the gear box ratio (as defined in Eq. (8)), $DSlead$ is the drive screw lead in meters/revolution, η_{ds} is the efficiency of the drive screw (which is 0.9 in forward drive and 0.8 in back drive for ballscrews [8]), F_{load} is the external axial load acting on the drive screw in N, and m is the total mass of the drive screw nut and external load in kg.

Optimal Speed/Position Controller with Constraint

To maximize motor performance while satisfying the desired residual lifetime, we consider using standard LQ optimal control design for speed/position tracking control, while a lifetime-dependent constraint (e.g., maximum allowable motor current) is imposed externally on the LQ optimal controller.

Following standard LQ optimal control design procedure, our objective is to minimize the performance index (cost function) given by

$$\mathsf{P} = \frac{1}{2} P(X(t_f) - X^*(t_f))^2 + \frac{1}{2}\int_o^{t_f} (Q(X - X^*)^2 + ru^2)dt \tag{15}$$

where

$$X^* = \begin{bmatrix} x_1^*(t) \\ x_2^*(t) \end{bmatrix} = \begin{bmatrix} \theta_r^*(t) \\ \omega_r^*(t) \end{bmatrix}, \; t_o \le t \le t_f \tag{16}$$

is the reference (desired) trajectory for the motor angular position and speed, and

$$P = P^T = \begin{bmatrix} p_{11} & p_{12} \\ p_{21} & p_{22} \end{bmatrix} \ge 0, \; Q = Q^T = \begin{bmatrix} q_{11} & q_{12} \\ q_{21} & q_{22} \end{bmatrix} \ge 0, \; r > 0 \tag{17}$$

are weighting factors.

For the motor given in Eqs. (9) – (12), the optimal control law is then obtained as [9]:

$$u = -KX + \frac{b^T v}{r} \tag{18}$$

where

$$K = [k_1 \quad k_2] = \frac{1}{r} b^T S \tag{19}$$

is the optimal feedback gain (Kalman gain) and b is defined in Eq. (12).

In Eqs. (18) and (19),

$$S = \begin{bmatrix} s_{11} & s_{12} \\ s_{21} & s_{22} \end{bmatrix}, \quad v = \begin{bmatrix} v_1 \\ v_2 \end{bmatrix} \tag{20}$$

are the solutions, respectively, to the Riccati and auxiliary input equations

$$-\dot{S} = A^T S + SA - Sbb^T S \frac{1}{r} + Q \ , \qquad S(t_f) = P \tag{21}$$

$$-\dot{v} = (A - bK)^T v + QX^* - Sd \ , \qquad v(t_f) = PX^* . \tag{22}$$

where A and d are defined in Eqs. (11) – (12).

The above LQ optimal controller can be extended to address constrained controller output by satisfying Pontryagin's minimum principle [9]:

$$H(X_{opt}, u_{opt}, \lambda_{opt}, t) \le H(X_{opt}, u, \lambda_{opt}, t) \tag{23}$$

for all admissible u, where

$$H(X, u, \lambda, t) = \frac{1}{2}(Q(X - X^*)^2 + ru^2) + \lambda^T (AX + bu + d) \tag{24}$$

is the Hamiltonian function. In Eq. (23), subscript *opt* denotes optimal quantities and λ is the costate vector. Inequality (23) then reduces to the following parabolic constraint:

$$\frac{1}{2} r u_{opt}^2 + \lambda_{opt}^T b u_{opt} \le \frac{1}{2} r u^2 + \lambda_{opt}^T b u \tag{25}$$

for all admissible u.

Inequality (25) implies that solution (18) is optimal as long as it remains within the admissible range of u. Otherwise, the optimal solution is given by either the upper or lower boundary of all admissible u, depending on which one is closest to solution (18). Thus, the next step is to specify the boundary of admissible u by taking into account the minimum required (desired) operational lifetime and predicted residual lifetime of the motor winding and bearing.

Computing Constraint Based on Desired Winding Lifetime

From Eqs. (1) and (2), the relationship between the lifetime of brand new winding *Life*(t) and the predicted residual lifetime of used winding *Liferes*(t) can be written as

$$Life(t) = \frac{Liferes(t)}{1 - \int_o^t \frac{d\tau}{Life(\tau)}} \ , \quad t_o \le \tau < t \tag{26}$$

Since we want to ensure the predicted residual lifetime is greater than or equal to the desired residual lifetime at any given time instant t, we can rearrange Eq. (26) as the following constraint:

$$Life(t) \ge \frac{Lifedes(t)}{1 - \int_o^t \frac{d\tau}{Life(\tau)}} \ , \quad t_o \le \tau < t \tag{27}$$

where *Lifedes*(t) is the desired absolute residual lifetime for the winding. This constraint requires that we operate the winding at a sufficiently low temperature such that the lifetime of brand new winding corresponding to this temperature would satisfy Eq. (27). After computing the minimum required *Life(t)* from Eq. (27), the corresponding winding temperature $T_{wmax}(t)$ that yields *Life(t)* can then be obtained from Fig. 1 (by the use of inverse mapping). Note that $T_{wmax}(t)$ is the maximum allowable winding temperature at time instant t that will yield the desired residual lifetime.

Now the next step is to relate the maximum allowable winding temperature $T_{wmax}(t)$ to the maximum allowable amplitude of the controller output $|u_{max}(t^-)|$ (i.e., the motor torque current) at the previous time instant t^-. Here we define $t^- = t - \Delta t$, where Δt can be treated as a time step in simulation or a sampling period in the control implementation. Although the relationship between the winding temperature and motor current involves dynamic time lag, we can simplify the computation by considering the constant steady-state operation of the motor thermal circuit given in Fig. 2 (i.e., by setting the time-derivatives to zero in the dynamic equations of the thermal circuit). Furthermore, P_{loss} in Fig. 2 is approximated by the total copper losses [3], which are due mainly to the motor torque current. The relationship between the maximum allowable winding temperature at time instant t and the maximum allowable input current at time instant t^- can then be simplified as

$$\left| u_{max}(t^-) \right| = \sqrt{\frac{T_{wmax}(t) - T_{ambient}}{(R_{wc} + R_{ca})R_m}} \tag{28}$$

where R_m is the motor phase-to-phase winding resistance.

Due to the exponential asymptotic stability of the thermal circuit, as long as the winding temperature $T_{winding}(t^-)$ is less than or equal to $T_{wmax}(t)$ and

$$|u(t^-)| \le |u_{max}(t^-)| \tag{29}$$

is complied, the winding temperature will satisfy

$$T_{winding}(t) \le T_{wmax}(t) \ . \tag{30}$$

Note that Eq. (28) was derived based on constant steady-state operation and provides a conservative estimate on $|u_{max}(t^-)|$. During a dynamically varying speed trajectory, it is possible to apply a larger $u(t^-)$ than $|u_{max}(t^-)|$ without the winding temperature exceeding $T_{wmax}(t)$, particularly when $T_{winding}(t^-)$ is comfortably below $T_{wmax}(t)$. To improve the dynamic performance of the controller, one can then choose to disregard constraint (29) when $T_{winding}(t^-) < T_{wmax}(t)$. Specifically, when $T_{winding}(t^-) < T_{wmax}(t)$, we can let $u(t^-)$ be constrained only by the maximum available current of the motor drive or by the motor current limit, whichever is less.

Computing Constraint Based on Desired Bearing Lifetime

Motor bearing lifetime can be controlled by constraining either the radial load on the bearing or the motor rotational speed. From Eqs. (3) – (5), the relationship between the radial load, rotational speed, and predicted bearing residual lifetime can be expressed by:

$$P_{eq}^3 \cdot \omega_r = 2\pi \cdot 10^6 \cdot C_r^3 \frac{1 - \int_{t_o}^{t} \frac{d\tau}{L_{10}(\tau)}}{L_{10res}(t)}, \quad t_o \le \tau < t \tag{31}$$

where $L_{10res}(t)$ is in seconds.

Consider the motor shown in Fig. 3. In general, the bearing closer to the load side (closer to the gearbox) experiences heavier load. Thus, control of bearing lifetime will focus on bearing #2 shown in the figure.

The radial load acting on bearing #2 can be expressed by

$$P_{eq} = W_r \frac{l_1 + l_2}{l_1} \tag{32}$$

where W_r is the total radial force at the gear mesh, and l_1 and l_2 are the lengths defined in Fig. 3. The total radial force at the gear mesh is comprised of two components:

$$W_r = \sqrt{W_t^2 + W_r'^2} = \sqrt{W_t^2 + (W_t \cdot \tan(\gamma))^2} \tag{33}$$

where W_t is the tangential force at the gear mesh, W_r' is the separating force at the gear mesh, and γ is the gear pressure angle [10]. For spur gears, $\gamma = 20^\circ$, which results in

$$W_r = 1.0642 \cdot W_t = 1.0642 \cdot \frac{Trq}{r_G} \tag{34}$$

where Trq is the torque acting on the gear and r_G is the radius of the gear. Substitution of Eq. (34) into Eq. (32) yields

$$P_{eq} = cpeq \cdot Trq \tag{35}$$

where the coefficient for equivalent load is given by

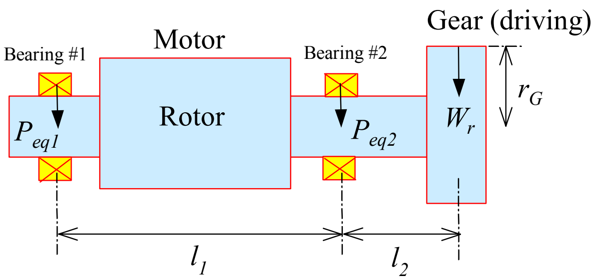

Figure 3 – Radial force acting on motor bearings.

$$cpeq = 1.0642 \frac{l_1 + l_2}{r_G \cdot l_1} \tag{36}$$

The torque acting on the gear can be assumed to be equal to the torque produced by the motor current, unless the external torque acting on the gear (e.g., from the load or disturbance) exceeds the torque produced by the motor current. Thus, under most conditions, Eq. (35) results in

$$P_{eq} = cpeq \cdot Trq = cpeq \cdot K_t u \tag{37}$$

where, u is the motor torque current.

Substituting Eq. (37) into Eq. (31) results in an equation that expresses the predicted bearing residual lifetime $L_{10res}(t)$ as a function of the motor current and motor rotational speed. We thus have the option of controlling the bearing lifetime by constraining either the controller output (i.e., the motor current) or the motor speed.

Since we want to ensure the predicted bearing residual lifetime is greater than or equal to the desired residual lifetime, i.e., $L_{10res}(t) \ge L_{10des}(t)$, we can rearrange Eq. (31) as the following constraint:

$$P_{eq}^3 \cdot \omega_r \le 2\pi \cdot 10^6 \cdot C_r^3 \frac{1 - \int_{t_o}^{t} \frac{d\tau}{L_{10}(\tau)}}{L_{10des}(t)}, \quad t_o \le \tau < t \tag{38}$$

Substituting Eq. (37) into (38), and then rearranging the resultant equation to express the constraint in terms of the controller output u, results in

$$|u(t)| \le \frac{1}{cpeq K_t} \left[\frac{2\pi \cdot 10^6 \cdot C_r^3}{\omega_r(t)} \cdot \frac{1 - \int_{t_o}^{t} \frac{1}{L_{10}(\tau)} d\tau}{L_{10des}(t)} \right]^{\frac{1}{3}}, \quad t_o \le \tau < t. \tag{39}$$

Eq. (39) gives the maximum allowable motor current based on the desired bearing residual lifetime $L_{10des}(t)$. We can also rearrange Eq. (39) to express the constraint in terms of a maximum bound on the motor speed $\omega_r(t)$. However, using the motor current constraint offers significant advantages over a motor speed constraint. Reducing the motor current to a constrained value can be enforced instantly, while, due to the time lag in the motor/gear dynamics, reducing the motor speed to a given value cannot occur instantly. Another advantage of using the motor current constraint for bearing lifetime control is that it can be easily combined with the motor current constraint derived for winding lifetime control. Thus, the motor controller can simultaneously control both winding and bearing lifetimes by simply enforcing the constraint

$$|u(t)| \leq \min \{ |u_{max}(t)|_{winding}, |u_{max}(t)|_{bearing} \} \quad (40)$$

where $|u_{max}(t)|_{winding}$ and $|u_{max}(t)|_{bearing}$ are the maximum allowable amplitudes of the motor current computed based on the desired winding lifetime and desired bearing lifetime, respectively.

Using the motor speed constraint for bearing lifetime control would be preferred in industrial applications where the motor operates at nearly constant speed and load. In this case, the speed constraint computed based on a desired bearing lifetime can simply be applied as the motor's commanded reference speed.

4. SIMULATION RESULTS

The proposed motor lifetime controller has been tested in simulation. The EMA and motor parameter values used in the simulation are shown in Table 1. Comparisons between the proposed lifetime controller (LQ optimal controller with output constraint), a standard PI controller, and a PI controller with output constraint are presented. The PI controller with output constraint applies the same lifetime-based motor current constraints as the LQ optimal controller. The initial desired winding lifetime $Lifedes(t_0)$ and desired bearing lifetime $L10des(t_0)$ are also shown in Table 1; the desired winding and bearing lifetimes decrease linearly with passing time.

EMA parameter	Value	Units
Rm	0.431	Ω
Rwc	0.425	°C/W
Rca	0.670	°C/W
Cwc	141.2	W·s/°C
Cca	895.5	W·s/°C
Twmax	100	°C
Tambient	25	°C
f_m	3.681e-5	N·m·s/rad
K_t	0.267	N·m/A
J_{mg}	8.8e-4	kg·m^2
J_{dsg}	1.6e-4	kg·m^2
m	0	kg
DSlead	0.00508	m/rev
G_{ratio}	5.20	–
η_{ds}	0.85	–
l_1	0.110	m
l_2	0.045	m
r_G	0.0635	m
cpeq	23.615	1/m
C_r	14946	N
$Lifedes(t_0)$	7680000	h
$L10des(t_0)$	19423659	h

Table 1 – EMA parameter values used in simulation.

Figure 4 shows the position trajectories of the BLDC motor resulting from the three types of controllers. Fig. 5 shows the position tracking errors. A demanding reference trajectory was selected for the simulation, in order to push the motor to its performance limit and highlight the effects of lifetime-based control. The EMA is assumed to be driving a spring load that generates an external force given by $F_{load} = (x/x_{max})\cdot F_{max}$ where x is the linear position of the EMA, x_{max} = 0.0762 m (3 inches) is the maximum linear position and F_{max} = 17792 N (4000 lbf) is the maximum value of the spring force.

We see from Figs. 4 and 5 that the standard PI controller (without constraint) provides the best position tracking performance, followed by the LQ optimal controller with constraint, and lastly the PI controller with constraint.

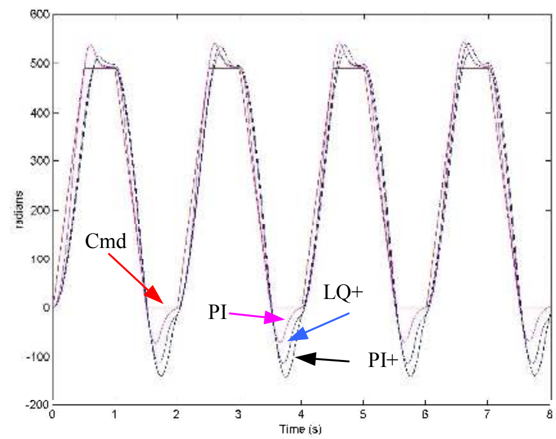

Figure 4 – Motor position trajectories. Comparing reference command (Cmd), standard PI control (PI), PI control with constraint (PI+), and LQ optimal control with constraint (LQ+).

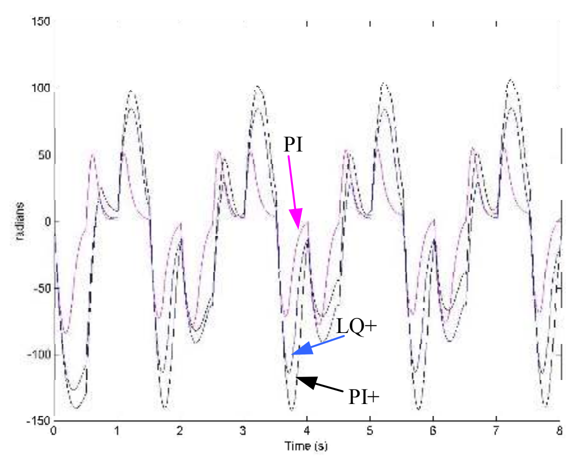

Figure 5 – Motor position tracking errors. Comparing standard PI control (PI), PI control with constraint (PI+), and LQ optimal control with constraint (LQ+).

Figure 6 shows the predicted percentage residual life of the motor winding resulting from the three types of controllers. The LQ optimal controller with constraint produced the highest residual life, followed by the PI controller with constraint, while the residual life resulting from the standard PI controller fell below the reference (desired) life. Although the PI controller with constraint is also capable of maintaining the desired residual life, its residual life and position tracking performance are both lower than those of the LQ optimal controller with constraint.

The winding temperatures resulting from the three types of controllers are shown Figure 7. The LQ optimal controller with constraint produced the lowest winding temperature, which confirms the longer life expectancy.

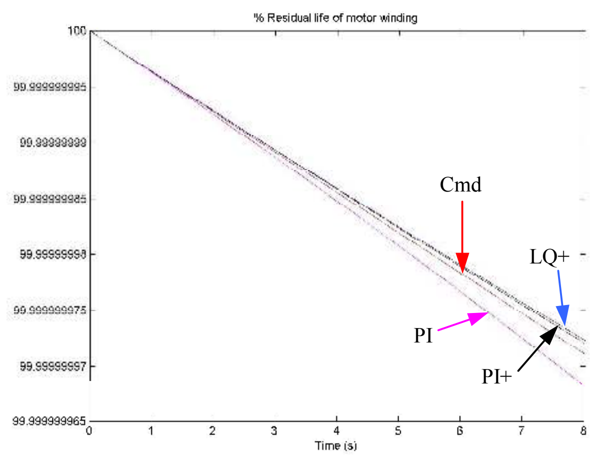

Figure 6 – Predicted motor winding percentage residual life. Comparing reference life (Cmd), standard PI control (PI), PI control with constraint (PI+), and LQ optimal control with constraint (LQ+).

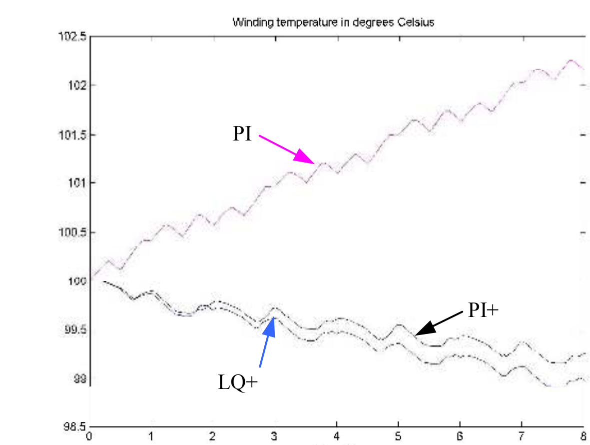

Figure 7 – Motor winding temperature in °C. Comparing standard PI control (PI), PI control with constraint (PI+), and LQ optimal controller with constraint (LQ+).

Figure 8 shows the motor bearing percentage residual lifetimes $\%L_{10res}$ resulting from the three types of controllers. The LQ optimal controller with constraint produced the highest residual life of the motor bearing, followed by the PI controller with constraint; the residual life resulting from the standard PI controller fell below the reference life.

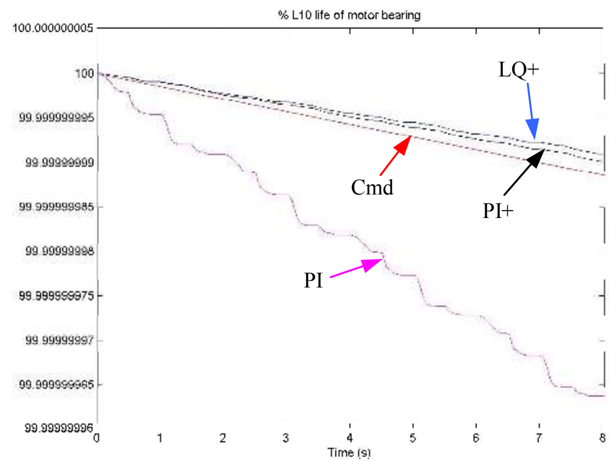

Figure 8 – Predicted motor bearing percentage residual life. Comparing reference life (Cmd), standard PI control (PI), PI control with constraint (PI+); and LQ optimal control with constraint (LQ+).

5. Conclusion

We introduced a new machinery control concept that incorporates desired lifetime into the control law. The ability to actively extend machinery lifetime will reduce maintenance cost and improve system safety and reliability. We explored the application of this concept to control the lifetime of the BLDC motor in an EMA. Our control methodology utilizes linear quadratic optimal control with output constraints. Specifically, the controller enforces the desired motor winding and bearing lifetimes as hard constraints on the motor current. In some situations, we may wish to violate the lifetime-based constraints in order to gain needed performance. One approach is to develop a high-level supervisory controller that gradually relaxes the desired lifetime when performance is deemed unsatisfactory. Alternatively, we can directly incorporate lifetime into the performance index for optimal control. We are currently investigating methods for achieving optimized trade-off between lifetime and performance.

Whether accurate lifetime control can be achieved is critically dependent on the accuracy of the models used in estimating residual life. In our derivations, we have used lifetime models established by winding and bearing manufacturers for constant operating conditions (i.e., constant temperature, constant load), and extrapolated these models for use in variable operating conditions by assuming that the damages incurred at each of the operating conditions are linearly additive. It is very likely that this assumption of linearly additive damage is too simplistic. Deriving an accurate damage model through physics-based modeling and experimental verification is a key area for future work.

REFERENCES

[1] L.U. Gökdere, S.L. Chiu and K.J. Keller, "Lifetime Control of EMAs," Integrated Systems Health Management (ISHM) Workshop, August 17-19, 2004, Air Force Research Lab, Dayton, Ohio.

[2] O. Moseler and R. Isermann, "Application of model-based fault detection to a brushless DC motor," *IEEE Trans. Industrial Electronics*, vol. 47, no. 5, pp. 1015-1020, October 2000.

[3] D. Kaiser, "Advances in digital servo drive motor protection," *Motion System Design*, pp. 21-25, June 2003.

[4] K.D. Hurst and T.G. Habetler, "A thermal monitoring and parameter tuning scheme for induction machines," Conference Record of the IEEE-IAS Annual Meeting, vol 1., pp. 136-142, 1997.

[5] E.V. Zaretsky, "A. Palmgren revisited—A basis for bearing life prediction," NASA TM-107440, Lewis Research Center, Cleveland, Ohio, April 1997.

[6] B.J. Hamrock and W.J. Anderson, "Rolling-element bearing," NASA Reference Publication 1105, 1983.

[7] T.J.E. Miller, *Brushless permanent-magnet and reluctance motor drives*. Oxford: Clarendon Press, 1989.

[8] http://roton.com.

[9] F.L. Lewis, *Optimal control*. New York: John Wiley & Sons, 1986.

[10] Reliance Gear Company Limited, *Bearing load calculations*.www.reliance.co.uk/products/downloads/chapters/bearings.pdf.

BIOGRAPHY

Levent U. Gökdere is a Research Scientist at Rockwell Scientific. He received a Ph.D. in Electrical Engineering from the University of Pittsburgh, PA in 1996. From 1996 to 2000, he was employed as a Post-Doctoral Research Associate for the Virtual Test Bed (VTB) project at the University of South Carolina. As a team member of the VTB, he developed simulation models for power electronic circuits and large-scale electric power distribution systems with an emphasis on naval ships. Since November 2000, he has been working at Rockwell Scientific Company. His current research interests include health prognostics and control of electric machines, and modeling, simulation, and testing of power electronic converters.

Stephen Chiu is Manager of the Control & Power Systems department at Rockwell Scientific. He received a double BS degree in Mechanical Engineering and Nuclear Engineering from U.C. Berkeley in 1983 and a MS degree in Mechanical Engineering from MIT in 1985. He joined Rockwell Scientific in 1985, which was then the corporate research lab of Rockwell International. At Rockwell Scientific, he performed research in robotics, intelligent control, and data mining, and later transitioned into project management roles. His current research interests are machinery health prognostics and adaptive control based on machinery health.

Kirby Keller is a Technical Fellow for the Boeing Company. He has 30 years experience in the application of intelligent systems to air and space vehicles. His current duties include technical leadership and project management for the Integrated Vehicle Health Management (IVHM) program within the Advanced Support Concepts Thrust of Boeing Phantom Works, which is chartered with developing and transitioning technology to Boeing products across the enterprise. He holds a Ph. D. in Mathematics from Iowa State University and is the author of over 40 technical papers, conference presentations, and technical reports.

John Vian is a Technical Fellow at The Boeing Company. He received a B.S. in Mechanical Engineering from Purdue University in 1981, and an M.S. in Aeronautical Engineering and Ph.D. in Electrical Engineering from Wichita State University in 1986 and 1991. His experience is in safety-critical decision and control systems, modeling and simulation, and systems health management. He has supported flight control design on KC-135, Boeing Robotic Air Vehicles, DARPA STOVL Aircraft, and Boeing 777 programs, and has served as Principal Investigator on multiple research contracts. He currently leads Boeing Phantom Works' vehicle health management enabling technology program.